JOURNAL OF CATALYSIS 15, 153–162 (1969)

Kinetics and Catalyst Deactivation in 1-Butene Dehydroisomerization over Chromia–Alumina

L. FORNI, L. ZANDERIGHI

From the Istituto di Chimica Fisica Università di Milano

C. CAVENAGHI

From the Società Italiana Resine, Milano, Italy

AND

S. CARRÀ

From the Istituto di Chimica Fisica Università di Messina

Received February 18, 1969; revised April 9, 1969

A kinetic study of 1-butene dehydroisomerization over chromia–alumina at 510, 530, and 550°C is reported. The kinetics of cracking side-reactions has been also investigated. The coke deposition has been analyzed with a microbalance flow reactor system. A complete kinetic scheme has been formulated, taking into account both dehydroisomerization and coke formation reactions.

Introduction

In a previous paper (*1*) a kinetic study of *n*-butane dehydrogenation reaction over chromia–alumina has been reported. Such a research has been successively extended to 1-butene and the results are given in the present work, in which the kinetics of both dehydrogenation and isomerization processes have been studied in a temperature range between 510 and 550°C. These reactions take place together with cracking side reactions, leading to coke deposition on the catalyst surface, and to a consequent progressive deactivation. These side reactions are more notable with an olefinic than with a paraffinic feed, so that a careful examination of the influence of such processes on the dehydroisomerization reactions became necessary. This study allowed us to formulate a complete kinetic scheme, by which both dehydroisomerization and coke formation processes are taken into account.

Experimental Methods

Materials. 1-Butene was a "pure grade" Phillips Petroleum Co. product. Its purity, tested by gas chromatography, was >99.5%, the remaining part being *n*-butane with traces of propane and propylene. Nitrogen was >99.999% pure. The catalyst, previously described (*1*), was 20–40 mesh alumina impregnated with 10% (wt) chromia.

Equipment. The dehydroisomerization runs were conducted in the previously described (*1*) stainless steel tubular flow reactor.

Procedure. All runs were performed with fresh catalyst as follows: after the weighed quantity of catalyst had been introduced into the catalyst basket, the reactor was flushed with a small nitrogen flow (50 ml/min) to eliminate oxygen. During this flushing the reactor temperature was raised up to 100°C below the chosen reaction temperature and at this point the feeding of gas mixture (1-butene and nitrogen) at the desired flow rates and ratios was started. After stationary conditions were obtained (during next 0.5 hr), three samples of reacted gases were taken at every 0.5 hr. In Table 1 a typical run analysis is given.

Some runs were performed with the aim

TABLE 1
TYPICAL RUN ANALYSIS

Temp (°C)	550
P_A (atm)	0.181
1-Butene feed rate (ml/min)	42.5
Nitrogen feed rate (ml/min)	195.5
Outgoing gas flow rate (ml/min)	235.8
1-Butene:nitrogen feed ratio	1:4.5
Catalyst wt (g)	1.000
Outgoing gas analysis (% by vol)	
Nitrogen + hydrogen + methane	83.555
Ethane + ethylene	0.100
Propane	Traces
Propylene	0.095
n-Butane	0.070
1-Butene	8.310
trans-2-Butene	3.820
cis-2-Butene	3.050
Butadiene	1.000

of determining the catalyst resistance to the fouling and have been conducted in the same way, but for a period of time up to 7 hr, taking samples every 0.5 hr.

In a last run the reacting gases were passed over a catalyst sample placed on the pan of a Cahn microbalance, working at the temperature of 510°C and 1-butene partial pressure at the feed of 0.250 atm, determining the increase in weight of catalyst due to coke formation. This run has been conducted for over 14 hr.

Analysis. The analysis of the gases entering and leaving the reactor was performed by gas chromatography, as previously described (*2*).

RESULTS

A set of runs have been performed at 510, 530, and 550°C and at different 1-butene partial pressures, ranging from 0.071 to 0.250 atm, and the results are graphically shown in Figs. 1–5. The results of "long" runs are graphically shown in Figs. 6, 7. The deactivation run, performed with the Cahn balance, is shown in Fig. 8.

From the increase in weight of catalyst with time, a mean value of about 2.5×10^{-4} moles/hr g cat for butene cracking reaction rate has been calculated. On the other hand the mean value of 1-butene disappearance rate, due to isomerization and dehydrogenation, was about 0.15 moles/hr g cat.

REACTION KINETICS

Influence of cracking. The influence of cracking reactions on dehydroisomerization reactions may be evaluated by means of a material balance on a small catalyst volume element dV_R of cross section A and thickness dz. Applying the continuity equation we have:

$$\left[Fx - F\left(x - \frac{\partial x}{\partial z}\,dz\right)\right] dt_c = dV_R\,\alpha\,\frac{\partial x}{\partial t}\,dt_c + dV_R\,dt_c r_s, \quad (1)$$

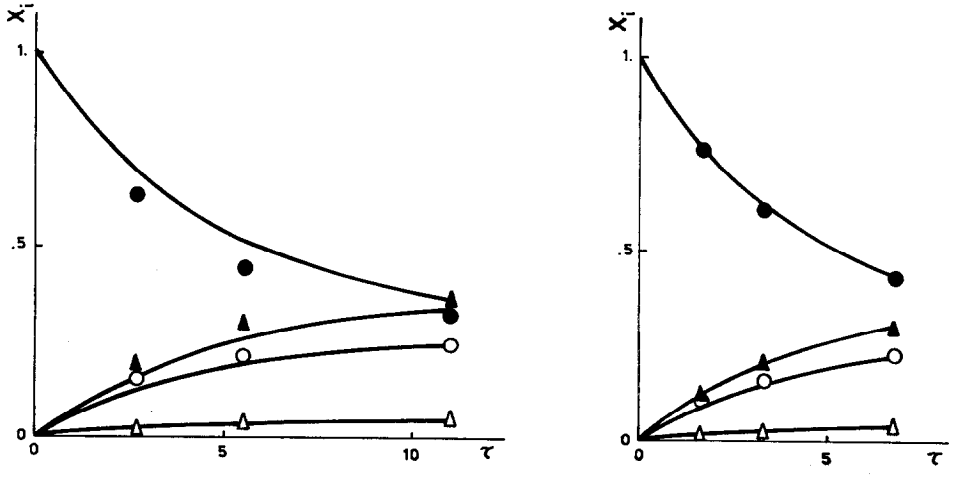

FIG. 1. Reaction of 1-butene at 510°C: (left), P_A = 0.071 atm; (right), P_A = 0.111 atm. (●), 1-butene; (▲), *trans*-2-butene; (○), *cis*-2-butene; (△), butadiene; (—), calculated from Eqs. (5).

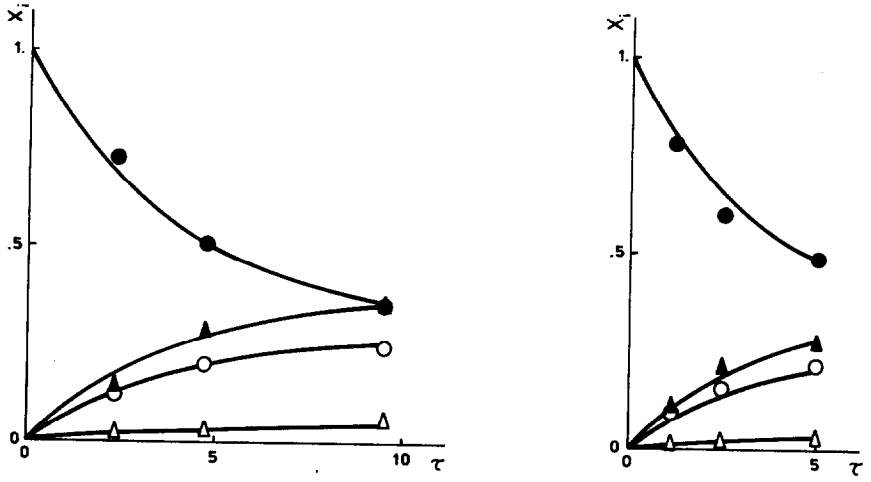

FIG. 2. Reaction of 1-butene at 510°C: (left), P_A = 0.181 atm; (right), P_A = 0.250 atm. Symbols and solid lines as in Fig. 1.

where F is the 1-butene feeding flow rate (moles/hr); x the 1-butene molar fraction, referred to 1 mole of fed olefin; α the ratio: moles of 1-butene/total volume at the feed; r_s the rate of coke formation (hydrocarbon cracked moles/hr catalyst volume); t_c the time (hr) that 1-butene molecules are in contact with the catalyst. Dividing by $dV_R = A\,dz$ we have:

$$\frac{F}{A}\frac{\partial x}{\partial z} = \alpha\frac{\partial x}{\partial t_c} + r_s. \qquad (2)$$

The first term of the right member in Eq. (2) gives the disappearance of 1-butene in the volume element dV_R, due to all reactions, except coke formation reactions. At 510°C, on the basis of experimental results obtained with the microbalance, such term was some 600 times greater than the second term, so that we can neglect the second with respect to the first and write:

$$t_c = \frac{\alpha A z}{F} = \frac{V_R \alpha}{F} = \tau\frac{\alpha}{\rho_{cat}} \qquad (3)$$

where $\tau = W/F$ is the time factor of the olefin, being W the catalyst weight in grams and F the 1-butene feeding rate in moles/hr; V_R the catalyst volume (cm³) and ρ_{cat} the catalyst density (g/cm³). Equation (3) gives a relationship between the time t_c and the

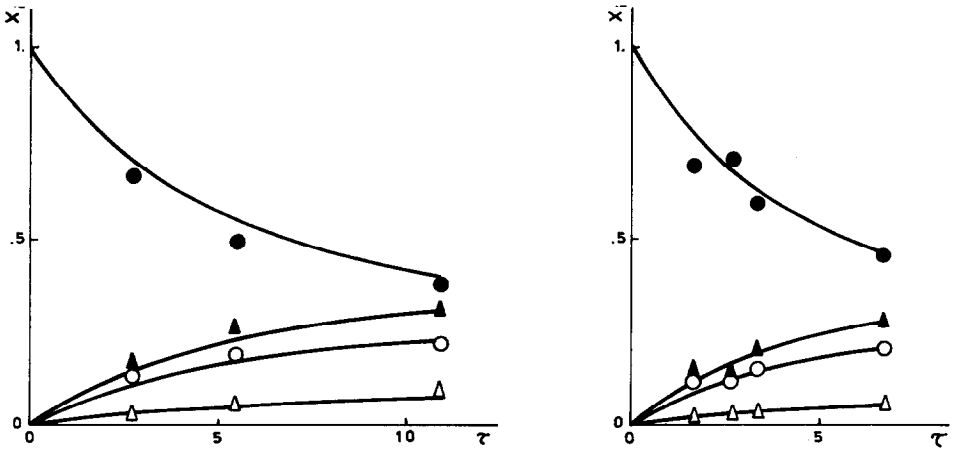

FIG. 3. Reaction of 1-butene at 530°C: (left), P_A = 0.071 atm; (right), P_A = 0.111 atm. Symbols and solid lines as in Fig. 1.

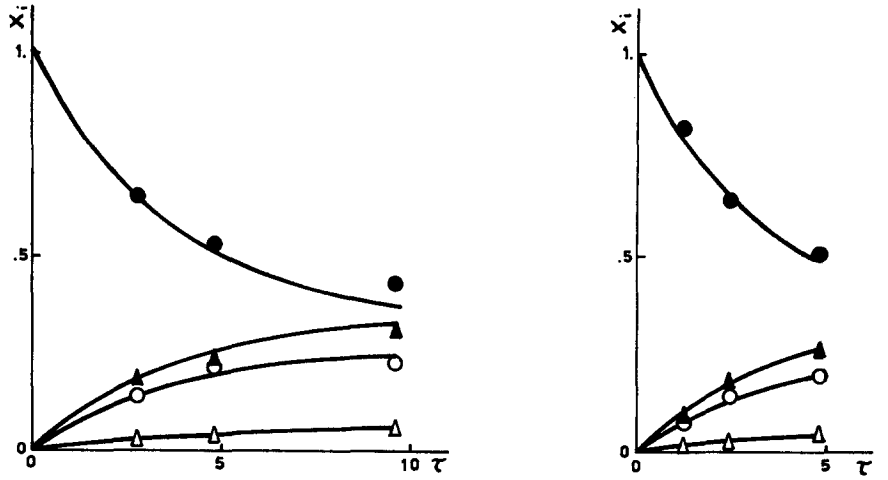

FIG. 4. Reaction of 1-butene at 530°C: (left), P_Δ = 0.181 atm; (right), P_Δ = 0.250 atm. Symbols and solid lines as in Fig. 1.

time factor τ. Even for the runs performed at the highest butene concentration (partial pressure = 0.250 atm), the value of τ was about 3×10^5 t_c. Since the highest time factor for flow reactor runs was τ = 15 hr g cat/moles, the catalyst fouling corresponded to a time not exceeding $t_c = 5 \times 10^{-5}$ hr. Therefore catalyst fouling, for flow reactor runs (Figs. 1–5) may always be neglected, except for a minor effect which takes place when the reactor is going to reach stationary conditions. For this reason special care was taken in reaching the steady state always by rigorously constant conditions, so that the collected kinetic data would be perfectly comparable.

Kinetical analysis. The general scheme of 1-butene dehydroisomerization reactions may be represented as shown in Fig. 9. The reaction kinetics is then expressed by the following equations:

$$
\begin{aligned}
-\frac{dx_1}{d\tau} &= r_{12} + r_{13} + r_{14} - r_{21} - r_{31}, \\
-\frac{dx_2}{d\tau} &= r_{21} + r_{23} + r_{24} - r_{12} - r_{32}, \\
-\frac{dx_3}{d\tau} &= r_{31} + r_{32} + r_{34} - r_{13} - r_{23}, \\
\frac{dx_4}{d\tau} &= r_{14} + r_{24} + r_{34}, \qquad (4)
\end{aligned}
$$

where x_i are the molar fractions, referred to the fed olefin, of the substances shown in Fig. 9 and r_{ij} are the rates of transformation of the ith substance in the jth one.

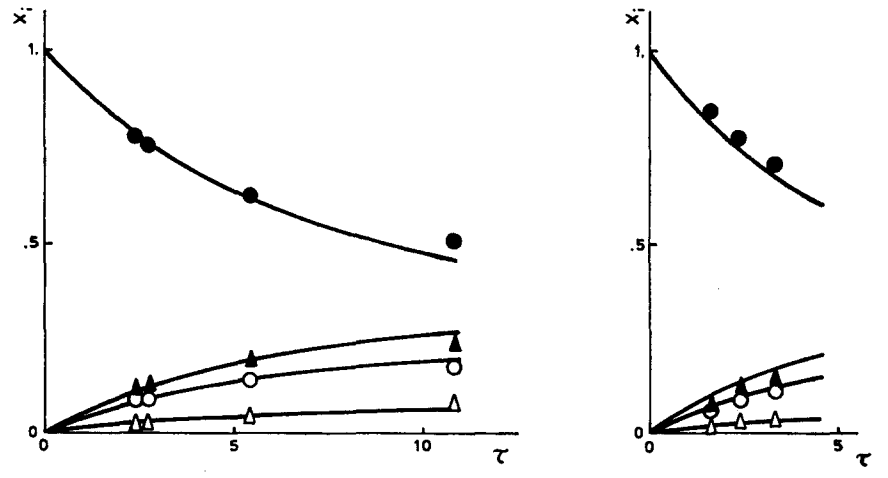

FIG. 5. Reaction of 1-butene at 550°C: (left), P_Δ = 0.071 atm; (right), P_Δ = 0.111 atm. Symbols and solid lines as in Fig. 1.

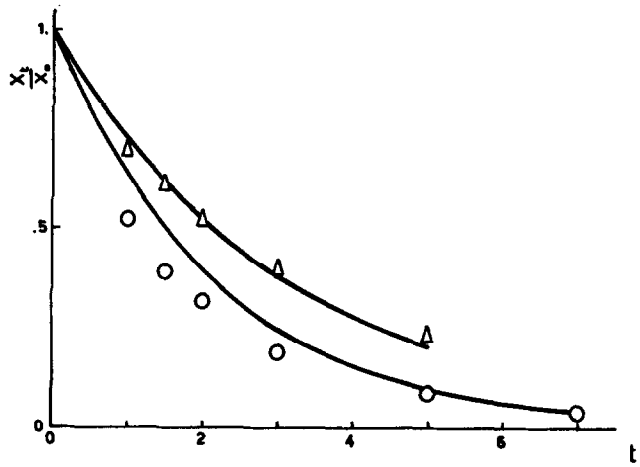

FIG. 6. Change in 1-butene conversion vs. reaction time (hr): T = 530°C; (△), 0.071 atm; (○), 0.250 atm; (—), calculated from Eq. (20).

Following the Langmuir-Hinshelwood model for monomolecular reactions, on the basis of previous works (*1*, *2*), we assumed that the rate determining steps are the surface reactions, with a single-site mechanism for the isomerization reactions and a dual-site mechanism for dehydrogenation. Equations (4) then become:

where: $A = 1/(1 + x_4 + c)$ and $B = b_\Delta(x_1 + x_2 + x_3) + (b_D + b_H)x_4$, being b_Δ the adsorption equilibrium constant of butenes (atm^{-1}), assumed the same for the three isomers; b_D and b_H the adsorption equilibrium constants (atm^{-1}) of butadiene and hydrogen; c the molar ratio between inert

$$
\begin{aligned}
-\frac{dx_1}{d\tau} &= b_\Delta \cdot A \left\{ \frac{1}{1 + B \cdot A} [(k_{12} + k_{13})x_1 - k_{21}x_2 - k_{31}x_3] + \frac{1}{(1 + B \cdot A)^2} k_{14}x_1 \right\}, \\
-\frac{dx_2}{d\tau} &= b_\Delta \cdot A \left\{ \frac{1}{1 + B \cdot A} [(k_{21} + k_{23})x_2 - k_{12}x_1 - k_{32}x_3] + \frac{1}{(1 + B \cdot A)^2} k_{24}x_2 \right\}, \\
-\frac{dx_3}{d\tau} &= b_\Delta \cdot A \left\{ \frac{1}{1 + B \cdot A} [(k_{32} + k_{31})x_3 - k_{13}x_1 - k_{23}x_2] + \frac{1}{(1 + B \cdot A)^2} k_{34}x_3 \right\}, \\
\frac{dx_4}{d\tau} &= \frac{b_\Delta \cdot A}{(1 + B \cdot A)^2} [k_{14}x_1 + k_{24}x_2 + k_{34}x_3],
\end{aligned}
\tag{5}
$$

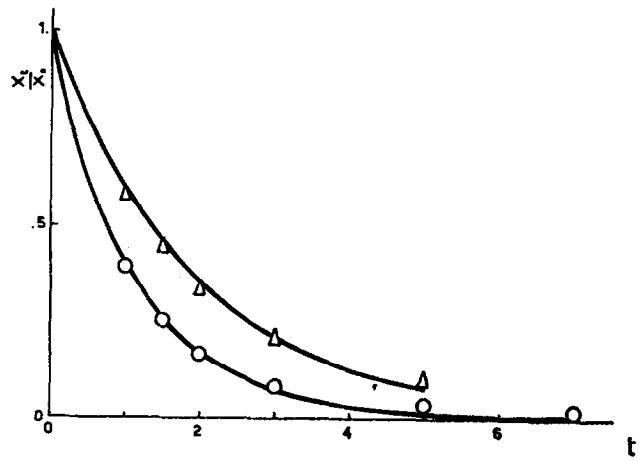

FIG. 7. Change in 1-butene conversion vs. reaction time (hr): T = 550°C; (△), 0.071 atm; (○), 0.250 atm; (—), calculated from Eq. (20).

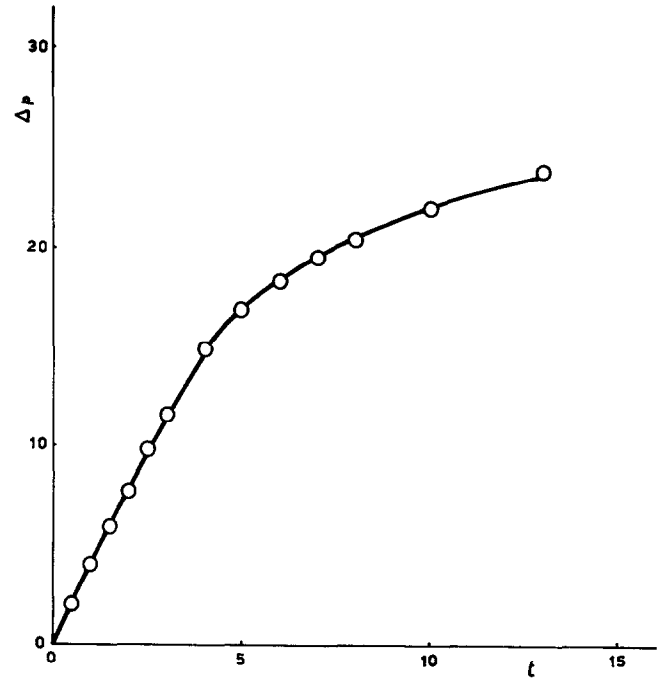

FIG. 8. Increase of catalyst weight with reaction time (hr); run performed with 0.161 g of fresh catalyst.

gas (nitrogen) and 1-butene at the feed; k_{ij} the reaction rate constants.

Reaction paths in triangular diagrams have been made for all the temperatures and an example is shown in Fig. 10. On the same diagram the equilibrium composition of the *cis/trans*-2-butene system (solid line), taken from literature data (*3*), is also drawn. One can see that experimental data lie on that line independently from the time factor and 1-butene partial pressure, so that the integration of Eqs. (5) has been done assuming that during the whole reaction time the *cis/trans*-2-butene system was at equilibrium. Such an integration was made numerically with the Runge-Kutta method, employing a UNIVAC 1108 computer. Then the following function

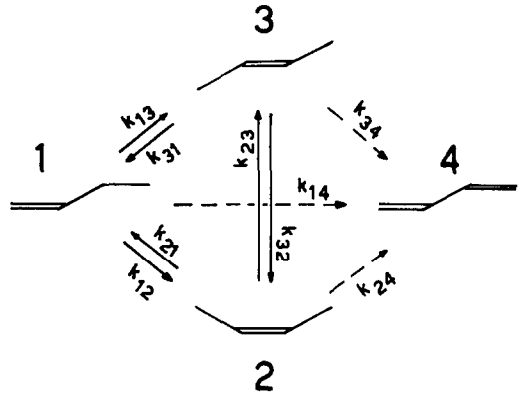

FIG. 9. Network of 1-butene isomerization and dehydrogenation reactions.

$$F_1(k_{ij},b_i) = \sum_{n=1}^{4}\left[\sum_{m=1}^{N}\left(\frac{|C_{n,m}-S_{n,m}|}{S_{n,m}}+\left|\frac{C_{n,m}-S_{n,m}}{C_{n,m}}\right|\right)\right] = \sum_{n=1}^{4}\sum_{m=1}^{N}\left(\frac{C_{n,m}^2-S_{n,m}^2}{S_{n,m}\cdot C_{n,m}}\right) \quad (6)$$

has been minimized with respect to the parameters k_{ij} and b_i by applying the steepest descent method. $C_{n,m}$ represents the calculated value of conversion at the mth run, performed at 1-butene partial pressure at the feed characterized by the subscript n, and $S_{n,m}$ represents the corresponding experimental value; N is the total number of runs. The application of such a method brings to a minimization of the sum of the differences between calculated and experimental conversions. Equation (6) revealed

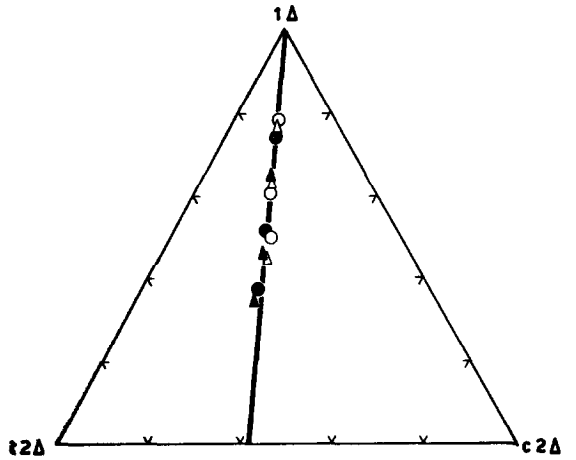

FIG. 10. Reaction paths of 1-butene dehydroisomerization reactions at 510°C, referred to the sum of three butenes only: (▲), 0.071 atm; (△), 0.111 atm; (●), 0.181 atm; (○), 0.250 atm; (—), the equilibrium composition of *cis/trans*-2-butene system.

useful for a fast convergency to the minimum of function F_1 (*5*). Since the minimization revealed to be quite insensitive to the difference between the dehydrogenation reaction rate constants of the three butenes, the same value has been attributed to such constants.

TABLE 2
REACTION RATE AND ADSORPTION EQUILIBRIUM CONSTANTS

T (°C)	510	530	550
b_Δ (atm^{-1})	40.0	18.0	10.0
$b_D + b_H$ (atm^{-1})	142.92	120.85	100.0
$k_{14} = k_{24} = k_{34}$ (moles/hr g cat)	0.0068	0.0151	0.0171
k_{12} (moles/hr g cat)	0.1096	0.1232	0.131
k_{13} (moles/hr g cat)	0.0918	0.1086	0.11

The results of the calculations are collected in Table 2. The agreement between calculated curves and experimental data is shown in Figs. 1–5. In Fig. 11 the plots of log b_Δ, log[1000 × ($k_{14} = k_{24} = k_{34}$)], log(10 × k_{12}), log(100 × k_{13}) vs. $10^3/T$ are reported. From the slopes and the intercepts of straight lines of Fig. 11 the values of apparent activation energies of 1-butene isomerization and dehydrogenation reactions and of standard enthalpies and entropies of *n*-butenes adsorption have been calculated. The values are reported in Table 3.

Catalyst deactivation. At 530 and 550°C and at 1-butene partial pressure of 0.071 and 0.250 atm some long runs have been performed, analyzing the reaction products every 0.5 hr for several hours. The results are graphically shown in Figs. 6, 7, in which the plots of the ratio X_t/X_0 vs. t are reported, being X_t the conversion that fouled catalyst gives at time t, and X_0 the conversion that fresh catalyst gives at $t = 0$.

TABLE 3
ACTIVATION ENERGIES OF REACTIONS AND ADSORPTION PARAMETERS

$\Delta E_{14}^{\neq} = \Delta E_{24}^{\neq} = \Delta E_{34}^{\neq}$	29.8 kcal/mole
$\Delta E_{12}^{\neq}$	5.7 kcal/mole
$\Delta E_{13}^{\neq}$	5.8 kcal/mole
ΔH_Δ^0	−44.5 kcal/mole
ΔS_Δ^0	−49.5 cal/mole °K

The rate of a catalytic reaction may be expressed as follows:

$$r = L_0 \Phi(P_i,T), \qquad (7)$$

being L_0 the number of active sites per unit mass of fresh catalyst and Φ a function of reacting gases partial pressures (P_i) and of temperature (T). If the catalyst deactivates, Eq. (7) becomes:

$$r = L_t \Phi(P_i,T), \qquad (8)$$

being L_t the number of active sites present at time t. In a first approximation, as proposed by Pozzi and Rase (*4*), we can write:

$$\frac{L_t}{L_0} \simeq \frac{X_t}{X_0}. \qquad (9)$$

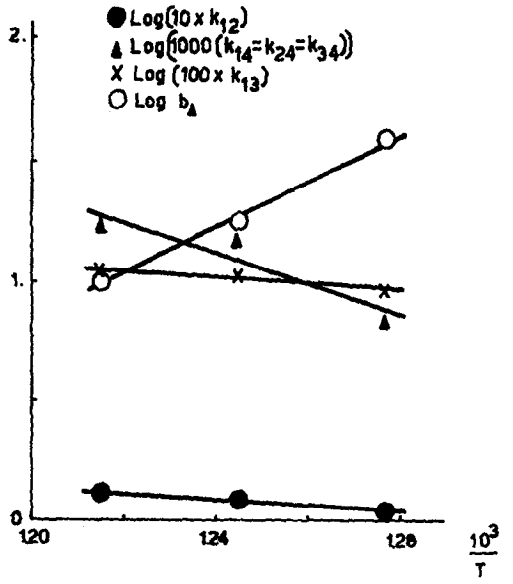

FIG. 11. Arrhenius plots of dehydroisomerization reactions: (○), log b_Δ; (▲), log[1000($k_{14} = k_{24} = k_{34}$)]; (●), log(10 × k_{12}); (X), log(100 × k_{13}).

Let us assume that the deactivation reaction takes place with the following mechanism:

$$B + \sigma \rightleftarrows B\sigma, \tag{10}$$

$$B\sigma \rightarrow Y\sigma + LG, \tag{11}$$

where B indicates the reacting substance and σ an active site. The first reaction represents the adsorption and the second one the deactivation, which takes place with formation of a deactivated site ($Y\sigma$) and light gaseous products (LG). Let ϑ_B be the fraction of active sites covered by the reagent B; ϑ_v the fraction of vacant sites; $\vartheta_t = \vartheta_v + \vartheta_B = L_t/L_0$ the fraction of nondeactivated sites at the time t and ϑ_y the fraction of deactivated sites. The rate of the surface reaction (11) will be expressed by:

$$\frac{d\vartheta_y}{dt} = k_y\vartheta_B, \tag{12}$$

being k_y the reaction rate constant. Assuming that the adsorption process (10) is at equilibrium, we have:

$$\frac{\vartheta_B}{P_\Delta\vartheta_v} = b_\Delta, \tag{13}$$

being b_Δ the adsorption equilibrium constant. Putting Eq. (13) in Eq. (12) we have:

$$\frac{d\vartheta_y}{dt} = k_y b_\Delta P_\Delta \vartheta_v. \tag{14}$$

The expression defining ϑ_t:

$$\vartheta_t = \vartheta_v + \vartheta_B, \tag{15}$$

by virtue of Eq. (13), becomes:

$$\vartheta_v = \frac{\vartheta_t}{1 + b_\Delta P_\Delta}. \tag{16}$$

But

$$\frac{d\vartheta_y}{dt} = -\frac{d\vartheta_t}{dt}, \tag{17}$$

so that, combining Eqs. (17), (14), and (16), we can write:

$$-\frac{d\vartheta_t}{dt} = k_y b_\Delta P_\Delta \frac{\vartheta_t}{1 + b_\Delta P_\Delta} = \beta\vartheta_t, \tag{18}$$

where $$\beta = \frac{k_y b_\Delta P_\Delta}{1 + b_\Delta P_\Delta}.$$

By integrating Eq. (18) we have:

$$\vartheta_t = \frac{L_t}{L_0} = e^{-\beta t}, \tag{19}$$

and, recalling Eq. (9),

$$\frac{X_t}{X_0} = e^{-\beta t}. \tag{20}$$

In applying Eq. (20), which gives the catalyst deactivation as a function of reaction time t, we gave to the adsorption equilibrium constant b_Δ, appearing in parameter β, the values of Table 2, corresponding to the adsorption equilibrium values of *n*-butenes. In such an approach the same adsorption equilibrium constants have been attributed also to butadiene, since its concentration was always low, with respect to that of butenes.

On the basis of Eq. (20) the deactivation curves, reported in Figs. 6, 7, have been correlated attributing to the constant k_y the following values:

T (°C)	k_y (hr^{-1})
530	0.59
550	1.13

The increase in catalyst weight due to coke deposition can be expressed by $\Delta p = a\vartheta_y$, being a the coke weight (mg) deposited at complete deactivation of active sites. Equa-

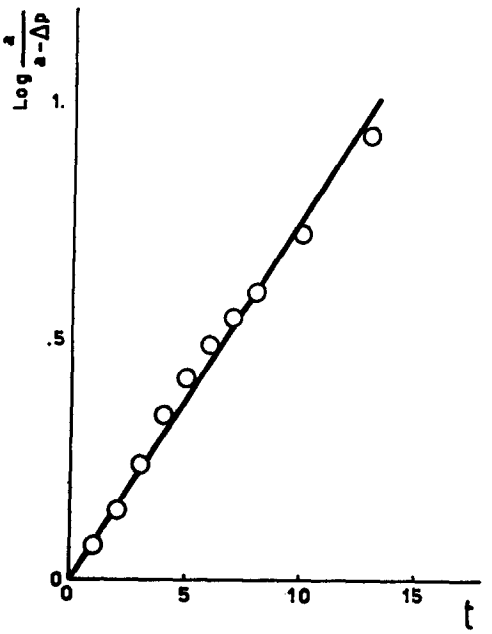

FIG. 12. Correlation of weight increase of catalyst by means of Eq. (23).

tion (18), by virtue of Eq. (17), may be written as:

$$\frac{d\vartheta_y}{dt} = \beta\vartheta_t = \beta(1 - \vartheta_y), \qquad (21)$$

or:

$$\frac{d\Delta p}{dt} = a\beta\left(1 - \frac{\Delta p}{a}\right), \qquad (22)$$

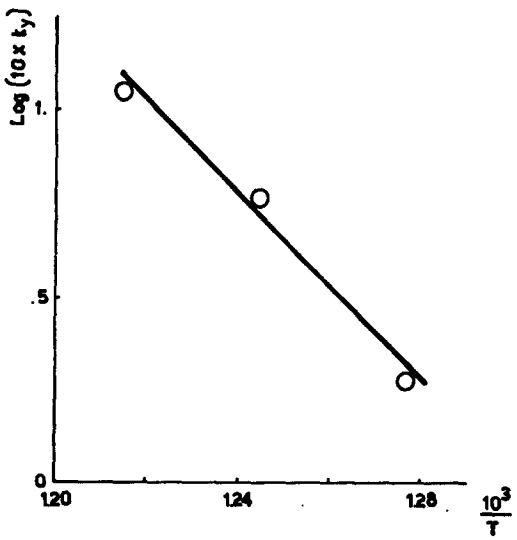

FIG. 13. Arrhenius plot of coke formation reaction.

and by integrating:

$$\log \frac{a}{a - \Delta p} = \frac{\beta}{2.303} t. \qquad (23)$$

Equation (23) was employed to interpret the increase in weight of catalyst during the run performed at 510°C with Cahn balance. Experimental data lie on a straight line on the logarithmic plot of Fig. 12, provided that a value of 27.1 is attributed to the constant a. From the slope of such straight line a value of 0.19 has been calculated for the constant β, from which a value of $k_y = 0.187$ hr^{-1} has been obtained. In Fig. 13 the Arrhenius plot for k_y is shown.

DISCUSSION

The kinetic scheme employed in the present work was adequate for the interpretation of the collected experimental data. Particularly some previous results (*1*, *2*) have been confirmed: namely that, while the isomerization reaction, for which the presence of a simple alumina surface is sufficient, follows a single-site mechanism, the dehydrogenation reaction, for which chromium ions are the active sites, follows a dual-site mechanism. Though the isomerization and dehydrogenation reactions occur on different active sites, we neglected the difference between the two 1-butene adsorption equilibrium constants. Actually such an approximation was wholly satisfactory.

A confirmation that these reactions tend to take place on different active sites comes out also from the fact that dehydrogenation reaction is more sensitive to deactivation due to coke formation than isomerization. For instance at 550°C and 1-butene partial pressure at the feed of 0.181 atm, for a reaction time of 3 hr, the decrease in conversion relative to isomerization reaction was 22%, while for dehydrogenation it was 37%.

Moreover, the coke formation reaction takes place, after adsorption of the olefin on the active sites, with a path parallel to that of the dehydroisomerization reactions. This fact was already found in a previous work (*6*) on the catalytic dehydrogenation of ethylbenzene to styrene.

It is worthwhile to speculate about the

mechanism of the deactivation process, due to coke formation. The value of constant a obtained from the correlation of Fig. 12 indicates that the increase of catalyst weight tends to a limiting value of 170 mg of deposed coke/g of catalyst, corresponding to a value of the order of 7×10^{-5} mg/cm^2 of catalyst surface. It is likely that the first step of olefin isomerization on alumina is the adsorption on sites on which there is at least a vacancy of a pair of oxide ions (*7*). In such sites a couple of exposed aluminum ions is present, one of them acting as a weak Lewis acid center for the olefin adsorption, and the other one helping the migration of a proton, that occurs during the isomerization reaction. A reasonable model of the hydrated γ-alumina surface (*8*) indicates the presence of one pair vacancy per about 200 Å^2 of surface. Previous researches on silica–alumina (*9*) showed that coke deposition occurs by formation of condensed ring aromatic structures. An infrared spectroscopic analysis (*9*) revealed a low hydrogen content, corresponding to a high degree of condensation toward a pseudographitic structure. In an ideal graphitic monolayer there is one carbonium atom per each 2.8 Å^2 (*10*). If the alumina surface would be covered by a uniform graphitic monolayer, 7.2×10^{-5} mg of C/cm^2 would be present. This value is quite close to the limiting value obtained from the run performed with the Cahn microbalance. Actually the coverage of the real alumina surface with coke should occur through the formation of different zones of multilayer graphitic areas and the poisoning of the catalyst seems to indicate that the formation of such areas preferentially takes place in correspondence of active centers.

Acknowledgment

The financial aid of Italian Consiglio Nazionale delle Ricerche is acknowledged.

References

1. Carrà, S., Forni, L., Vintani, C., *J. Catalysis* **9**, 154 (1967).
2. Forni, L., Zanderighi, L., and Carrà, S., *J. Catalysis*, **12**, 298 (1968).
3. Voge, H. H., and May, N. C., *J. Am. Chem. Soc.* **68**, 550 (1946).
4. Pozzi, A. L., and Rase, H. F., *Ind. Eng. Chem.* **50**, 7, 1075 (1958).
5. Zanderighi, L., unpublished work.
6. Carrà, S., and Forni, L. *Ind. Eng. Chem. Process Design Develop.* **4**, 281 (1965).
7. Gerberich, H. R., and Keith Hall, W., *J. Catalysis* **5**, 99 (1966).
8. Peri, J. B., *J. Phys. Chem.* **69**, 1, 220 (1965).
9. Eberly, P. E., Jr., Kimberlin, C. N., Jr., Miller, W. H., and Drushel, H. V., *Ind. Eng. Chem. Process Design Develop.* **5**, 193 (1966).
10. Pauling, L., "The Nature of the Chemical Bond," 3rd ed. Cornell Univ. Press, Ithaca, New York, 1960.